Supporting Information

Nickel-Thiolate Complex Catalyst Assembled in One Step in Water for Solar H_2 Production

Wei Zhang,[†] Jindui Hong,[†] Jianwei Zheng,[‡] Zhiyan Huang,[§] Jianrong (Steve) Zhou,[§] and Rong Xu*[,†]

[†]School of Chemical & Biomedical Engineering, Nanyang Technological University, 62, Nanyang Drive, 637459, Singapore

[‡]Institute of High Performance Computing, Agency for Science, Technology & Research, 1 Fusionopolis Way, #16-16 Connexis, 138632, Singapore

[§]School of Physical and Mathematical Sciences, Nanyang Technological University, Singapore 637371, Singapore

Experimental methods

Preparation of Ni-ME based molecular H_2 system and photocatalytic activity measurement. Visible light driven hydrogen evolution reactions were conducted in a closed gas circulation and evacuation system fitted with a top window Pyrex cell. In a typical reaction, nickel acetate (3 mM), 2-mercaptoethanol (30 mM) and Erythrosine B (2.25 mM) were added in sequence into a 100 mL of aqueous solution containing 15 vol% of TEOA under vigorous stirring. The pH value of the TEOA solution was prior adjusted to 8.5 using concentrated HNO_3. The light source was a 300 W Xenon lamp with a cut-off filter ($\lambda > 420$ nm). The reaction cell was kept at room temperature with a cooling water jacket. The produced hydrogen was detected using an online gas chromatography. Different longpass filters ($\lambda > 420$, 455, 475, 500 nm) and bandpass filters (centered at 420, 460, 530, 550 nm) were equipped when conducting reactions under photons of different wavelengths and collecting quantum efficiency results, respectively. The reaction solutions were irradiated under $\lambda > 420$ nm for 1 h before switching to bandpass filters during quantum efficiency measurement. The amount of hydrogen produced in the subsequent 5 h was used to calculate quantum efficiency using the equation below. The number of photons from irradiation was measured using a photodiode.

$$\text{QE} = \frac{2 \times \text{the number of evolved hydrogen molecules}}{\text{the number of incident photons}} \times 100\%$$

Materials characterization. The UV-visible absorption spectra were obtained on an UV-visible spectrophotometer (UV-2450, Shimadzu). Cyclic voltammetry experiments were performed on CHI 660D electrochemical station under a three-electrode cell system consisting of a glassy carbon working electrode, a Pt wire counter electrode and a saturated calomel reference electrode. Ni-ME complex in the solution was formed by adding 30 mM of nickel(II) acetate and 60 mM of ME in water. All measurements were carried out in aqueous solutions after purging of nitrogen thoroughly. The scan started at reduction with a rate of 100 mV/s for all measurements. All redox potentials are reported versus SCE. Electrospray ionization-mass spectrometry (ESI-MS) was used to analyze the photobleached dyes in the reaction solution and structure of nickel complexes. Mass spectra were recorded on a Thermo Finnigan LCQ Deca XP Max (San Jose, CA) ultra high sensitivity quadruple ion trap mass spectrometer fitted with Surveyor LC Auto Sampler and MS Pump. Data were recorded and processed using the X-Calibur software (Thermo Scientific, MA, USA).

Computational details. The structures of EB, Ni-ME (cyclic and linear) and Ni-MA complexes were constructed according to References 1 and were optimized by hybrid B3LYP functional together with a Lanl2dz basis set, in conjunction with a polarizable continuum model of solvation (PCM) using water as the solvent, as implemented in the Gaussian 09 program package. To save computational time, we used $Ni_4S_6C_{16}O_6H_{42}$ and $Ni_3S_4C_8O_8H_8$ clusters to represent Ni-ME and Ni-MA, respectively, to model the complex with EB. The structures of EB complex with Ni-ME or Ni-MA were constructed by considering the different orientations between EB and Ni-ME or Ni-MA. The structures with the lowest energy were taken for further analysis.

References 1:

(a) Lyday, P. A. *Iodine and Iodine Compounds*; Wiley-VCH: Weinheim, 2005. (b) Gould, R. O.; Harding M. M. *J. Chem. Soc. A Inorg. Phys.* **1970**, *6*, 875-881. (c). De Brabander, H. F.; Van Poucke, L. C.; Eeckhaut, Z. *Inorg. Chim. Acta* **1972**, *6*, 459-462. (d) Leussing, D. L.; Laramy, R. E.; Alberts, G. S. *J. Am. Chem. Soc.* 1960, *82*, 4826-4830

Full author list of Ref. 10c:

Frisch, M. J.; Trucks, G. W.; Schlegel, H. B.; Scuseria, G. E.; Robb, M. A.; Cheeseman, J. R.; Scalmani, G.; Barone, V.; Mennucci, B.; Petersson, G. A.; Nakatsuji, H.; Caricato, M.;

Li, X.; Hratchian, H. P.; Izmaylov, A. F.; Bloino, J.; Zheng, G.; Sonnenberg, J. L.; Hada, M.; Ehara, M.; Toyota, K.; Fukuda, R.; Hasegawa, J.; Ishida, M.; Nakajima, T.; Honda, Y.; Kitao, O.; Nakai, H.; Vreven, T.; Montgomery, Jr., J. A.; Peralta, J. E.; Ogliaro, F.; Bearpark, M.; Heyd, J. J.; Brothers, E.; Kudin, K. N.; Staroverov, V. N.; Kobayashi, R.; Normand, J.; Raghavachari, K.; Rendell, A.; Burant, J. C.; Iyengar, S. S.; Tomasi, J.; Cossi, M.; Rega, N.; Millam, N. J.; Klene, M.; Knox, J. E.; Cross, J. B.; Bakken, V.; Adamo, C.; Jaramillo, J.; Gomperts, R.; Stratmann, R. E.; Yazyev, O.; Austin, A. J.; Cammi, R.; Pomelli, C.; Ochterski, J. W.; Martin, R. L.; Morokuma, K.; Zakrzewski, V. G.; Voth, G. A.; Salvador, P.; Dannenberg, J. J.; Dapprich, S.; Daniels, A. D.; Farkas, Ö.; Foresman, J. B.; Ortiz, J. V.; Cioslowski, J.; Fox, D. J. Gaussian 09, Revision **A.1**, Gaussian, Inc., Wallingford CT, 2009.

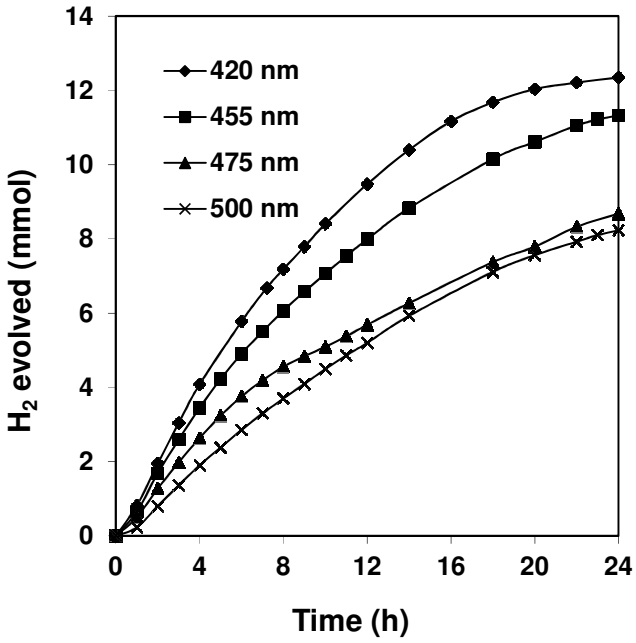

Figure S1. Time course of photocatalytic hydrogen evolution from the EB-Ni-ME system with a 300 W Xe lamp equipped with different long-pass cutoff filters at 420, 455, 475 and 500 nm.

UV-vis absorption analysis

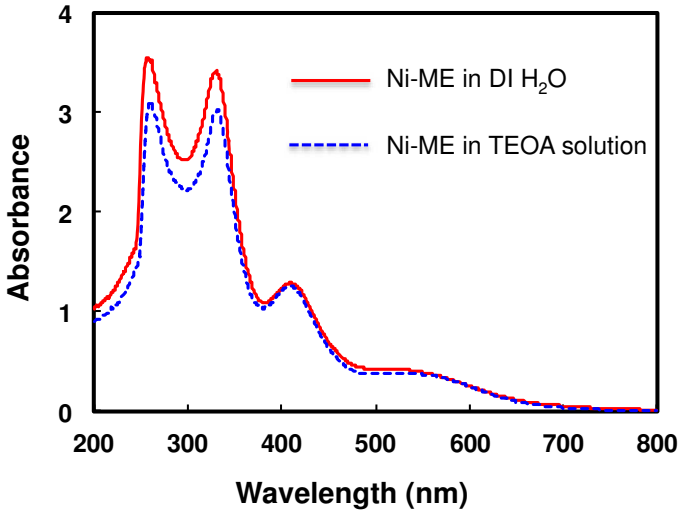

Figure S2. UV-vis spectra of Ni-ME complex in DI water (solid line, pH was adjusted to 8.5 using NaOH) and 5 vol% TEOA solution (dashed line, pH = 8.5). In both solutions, [Ni^{2+}] = 1 mM, Ni:ME = 1:10. DI water and 5 vol% TEOA solution were used as references, respectively. Compared to the reaction condition ([Ni^{2+}] = 3 mM, Ni:ME = 1:10, 15 vol% TEOA), the solution was 3 times diluted in order to avoid the oversaturation of the UV absorption peaks.

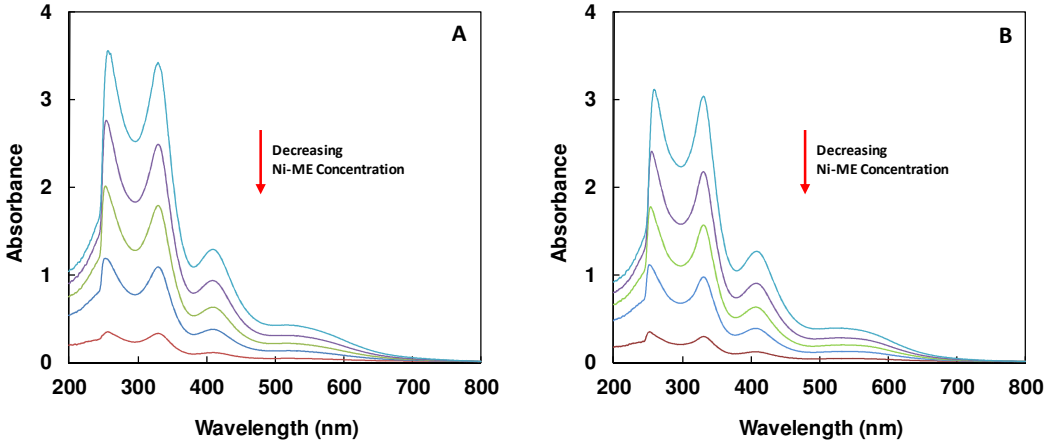

Figure S3. UV-vis spectra of Ni-ME complex in DI water (A) and in TEOA solution (B). Concentration of Ni^{2+} along the direction of arrow in both spectra: 1.0, 0.7, 0.5, 0.3, 0.1 mM.

Table S1 UV-vis absorption intensities of Ni-ME complex in DI water and TEOA solution with different Ni^{2+} concentrations (see Figure S3).

Solution		DI water				TEOA solution			
Peak Position		258 nm	330 nm	408 nm	525 nm	258 nm	330 nm	408 nm	525 nm
Ni Concentration (mM)	1	3.503	3.423	1.291	0.428	3.108	3.026	1.261	0.386
	0.7	2.751	2.472	0.93	0.306	2.402	2.14	0.894	0.272
	0.5	2.003	1.775	0.624	0.214	1.774	1.566	0.626	0.192
	0.3	1.172	1.078	0.372	0.128	1.111	0.969	0.38	0.115
	0.1	0.308	0.299	0.102	0.034	0.35	0.293	0.114	0.035

Table S2 The percentages of Ni-ME complex concentration in TEOA solutions against those in DI water at the same Ni^{2+} concentration.

Nickel Concentration (mM)	[Ni-ME] in TEOA/[Ni-ME] in DI H_2O
1.0	87.1%
0.7	87.9%
0.5	89.9%
0.3	92.4%
0.1	82.1%

A calibration line was obtained based on the absorption intensities at 330 nm of Ni-ME prepared in DI H_2O. The absorption intensities at 330 nm were used for calculation.

Electrospray ionization-mass spectrometry (ESI-MS) analysis

To elucidate the structure of Ni-ME complex and understand why the UV-vis absorption intensity of Ni-ME in TEOA is lower than that in water, positive ion electrospray ionization-mass spectrometry (ESI-MS) analysis was carried out for the following mixtures and the MS spectra are shown in Figure S4:

A: Ni-ME in water (pH adjusted to 8.5 by NaOH), dark brown color
B: Nickel acetate in TEOA solution (pH = 8.5), colorless
C: Ni-ME in TEOA solution (pH adjusted to 8.5 by NaOH), dark brown color

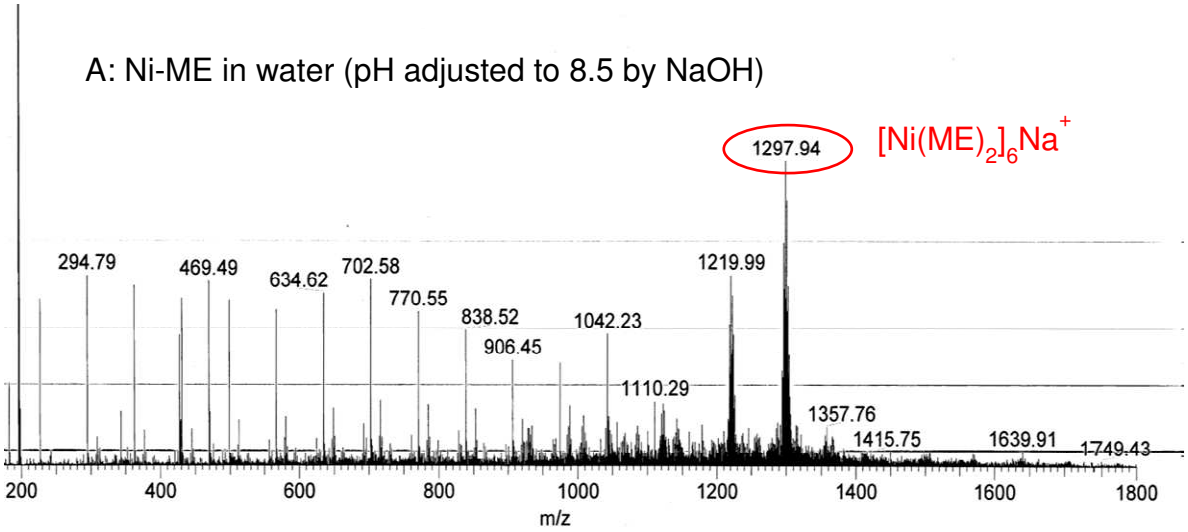

Figure S4A. ESI-MS spectrum of Ni-ME in water (pH adjusted to 8.5 by NaOH).

Table S3 Positive ion ESI-MS signals of Ni-ME complex prepared from different nickel sources in NaOH aqueous solution (pH=8.5), Ni^{2+}:ME = 1:10, [Ni^{2+}] = 3 mM.

Experiment	Nickel source	ESI-MS signal of the complex (m/z)
1	$Ni(Ac)_2$	1220.11, 1298.06
2	$Ni(NO_3)_2$	1220.09, 1298.04
3	$NiCl_2$	1220.23, 1297.78
4	$Ni(Ac)_2$ (KOH for pH adjust)	1237.09, 1314.01

(Atomic weight of H: 1.01, C: 12.01, O: 16.00, Na: 22.99, K: 39.10, S: 32.06, Ni: 58.69)

Discussion:
The results from Experiments 1-3 indicate that acetate is not involved in the formation of Ni-ME complex. The difference in m/z value (16) from 1 and 4 coincides with the difference in the atomic weight of Na and K. Hence it is suggested that Na^+ or K^+ is associated with the complex. Based on the above results, the Ni-ME complex in System A is $[Ni(ME)_2]_6Na^+$ (m/z = 1298.06). The signal at 1220 shall correspond to the complex with one ME (M.W. = 78) less, which could be most likely due to fragmentation of the complex under the harsh condition of ESI-MS.

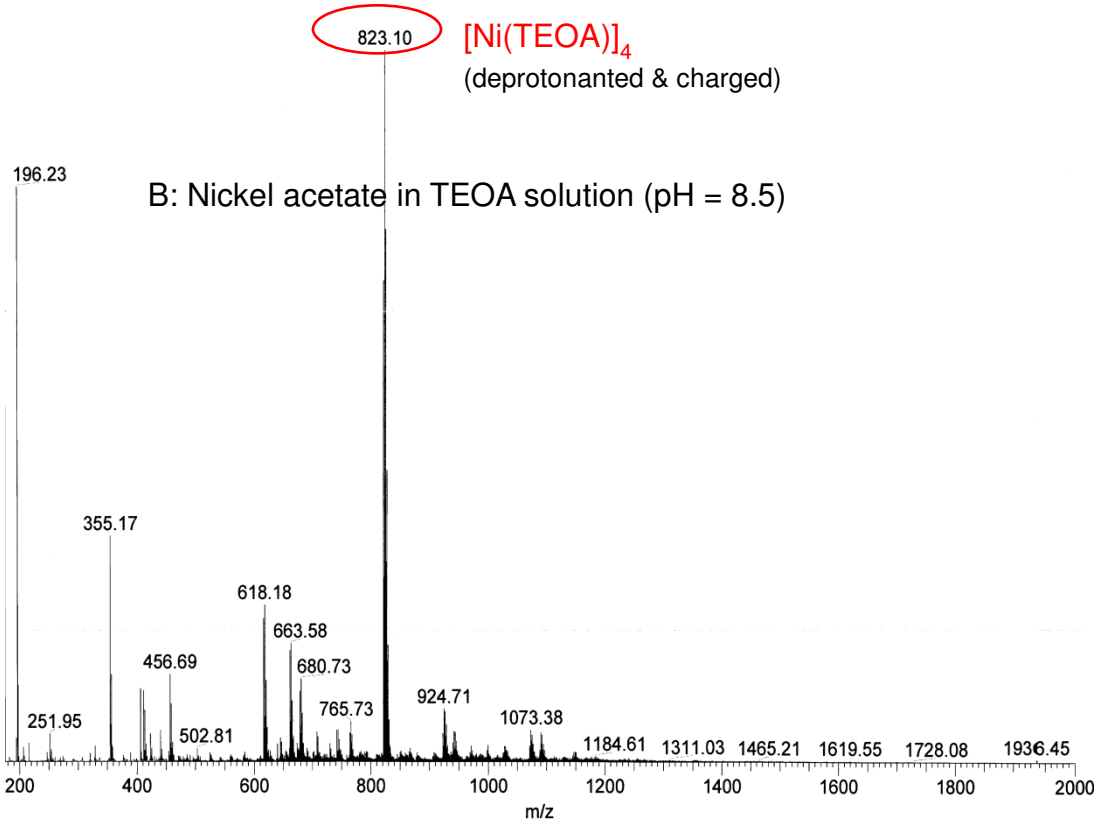

Figure S4B. ESI-MS spectrum of nickel acetate in TEOA solution (pH = 8.5).

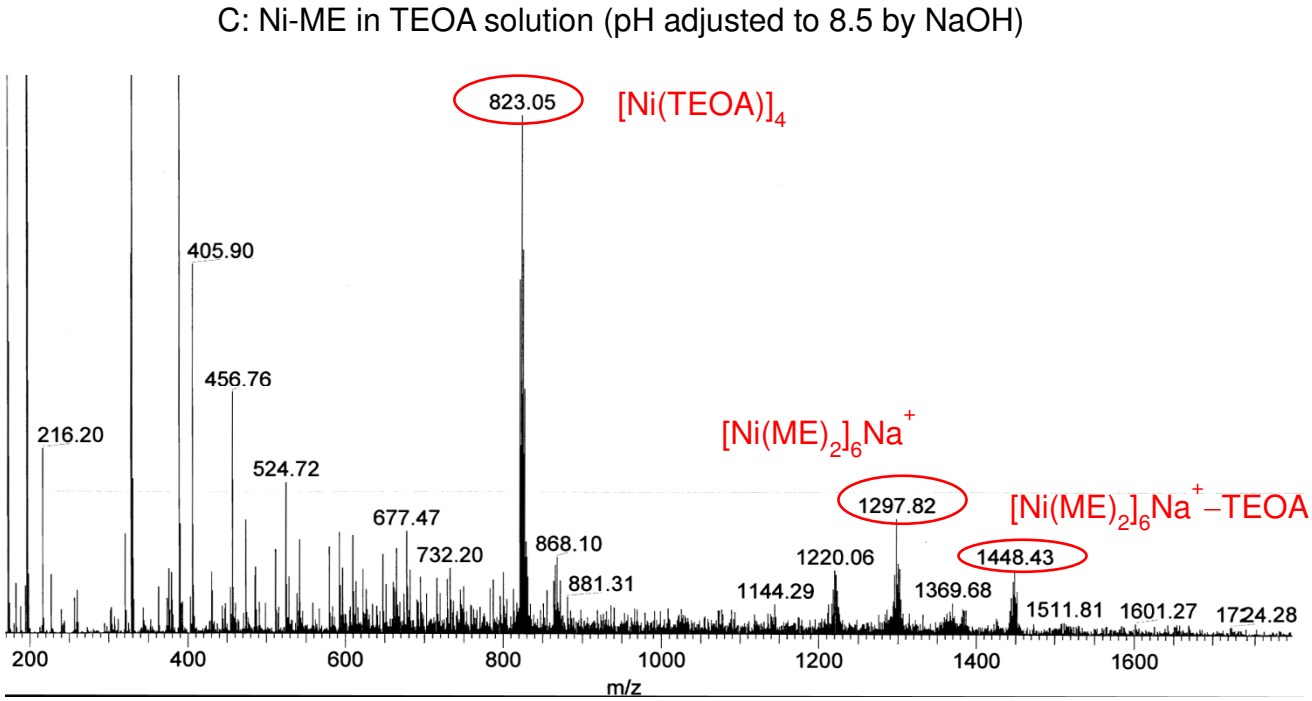

Figure S4C. ESI-MS spectrum of Ni-ME in TEOA solution (pH adjusted to 8.5 by NaOH).

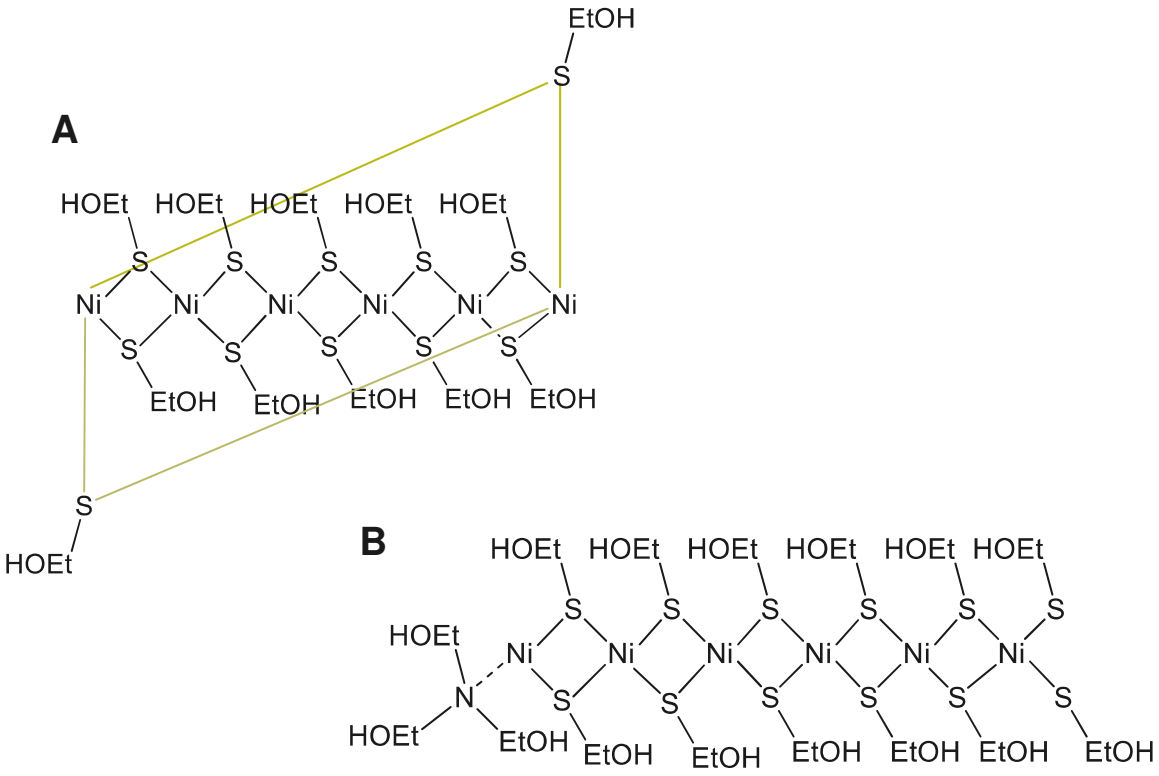

Figure S5. Proposed structure of cyclic hexameric Ni-ME complex (A) in aqueous TEOA solution, and possibly a liner structure (B) in equilibrium. Based on MS results, TEOA can be associated with the complex as proposed in (B).

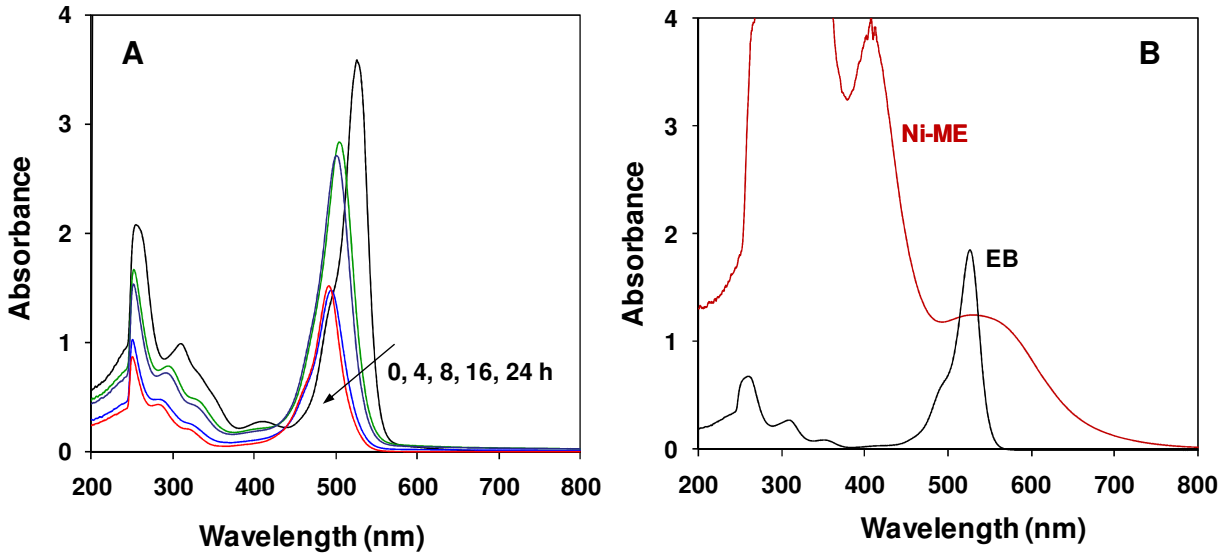

Figure S6. (A) Spectra of reaction mixture at 0, 4, 8, 16 and 24 h (along the arrow direction) of the reaction time. The reaction mixture was centrifuged and filtered before analysis. (B) UV-vis spectra of Ni-ME polymer complex (formed between 3 mM Ni^{2+} and 30 mM ME) and EB (50 ppm) in 15 vol% TEOA solution (15 vol% TEOA as reference).

Table S4 Relative dye molecule abundance in the reaction solution before irradiation and after 4, 8, 16 and 24 h of irradiation analyzed by ESI-MS.

Dye molecules (m/z)	EB (835.6)	EB-I* (709.6)	EB-2I (583.6)	EB-3I (457.6)	EB-4I (331.6)
	Relative Abundance				
Before reaction	100	0	0	0	0
After 4h	13	70	17	0	0
After 8h	0	0	70	30	0
After 16h	0	0	26	74	0
After 24h	0	0	16	16	68

*EB-I refers to EB dehalogenated with one iodide. EB-4I is EB dehalogenated with all iodide groups and becomes fluorescein.

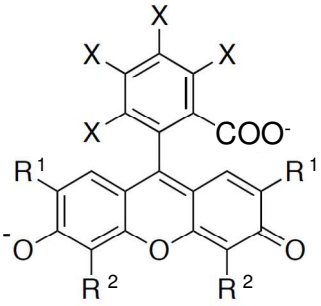

Erythrosin B	X = H, $R^1 = R^2 = I$
Erythrosin Yellowish	X = H, R^1 = I, R^2 = H
Rose Bengal	X = Cl, $R^1 = R^2 = I$
Eosin Y	X = H, $R^1 = R^2 = Br$
Fluorescein	X = H, R = H

Figure S7. Molecular structures of xanthene dyes investigated.

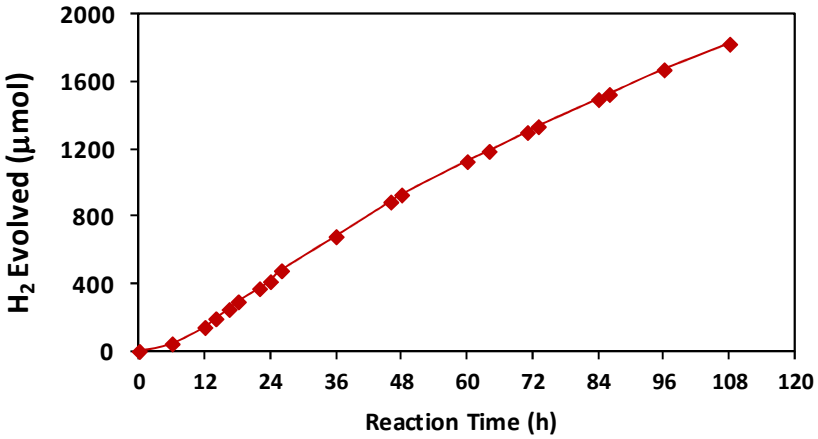

Figure S8. Continuous reaction of the Ni-ME catalyst for H_2 production using Fluorescein as the dye (2.25 mM) under visible light ($\lambda > 420$ nm).

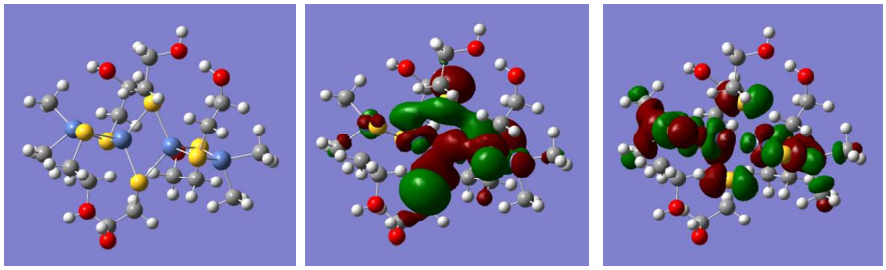

Figure S9. HOMO and LUMO orbitals in linear Ni-ME cluster.

Table S5 Mulliken charge in Ni-ME, Ni-MA and their complexes with EB in water.

	Cyclic Ni-ME	Ni-ME Cluster	Ni-MA	EB-Ni-ME*	EB-Ni-MA
Ni	-0.36	-0.16	0.33	0.14	0.47
Ni	-0.32	-0.24	-0.18	-0.05	0.23
Ni	-0.31	-0.24	0.33	-0.05	0.19
Ni	-0.33	-0.17		0.25	
Ni	-0.33				
Ni	-0.25				
S	0.06	0.02	0.25	-0.11	0.04
S	0.08	0.04	0.33	-0.12	0.10
S	0.08	0.04	0.34	-0.19	0.01
S	0.07	0.03	0.26	-0.23	0.01
S	0.09	0.03		-0.08	
S	0.10	0.06		-0.14	
S	0.06				
S	0.10				
S	0.08				
S	0.05				
S	0.04				
S	0.04				

*Linear cluster of Ni-ME was used for simulation.